Particle Tracking Microrheology of Lyotropic Liquid Crystals

ARTICLE *in* LANGMUIR · MAY 2011

Impact Factor: 4.46 · DOI: 10.1021/la200116e · Source: PubMed

2 AUTHORS, INCLUDING:

Mohammad Mydul Alam
KSP
24 PUBLICATIONS **216** CITATIONS

SEE PROFILE

Langmuir

ARTICLE

pubs.acs.org/Langmuir

Particle Tracking Microrheology of Lyotropic Liquid Crystals

Mohammad Mydul Alam and Raffaele Mezzenga*

ETH Zurich, Food & Soft Materials Science, Institute of Food, Nutrition, & Health, Schmelzbergstrasse 9, LFO, E 23, 8092 Zürich, Switzerland

Supporting Information

ABSTRACT: We present comprehensive results on the microrheological study of lyotropic liquid crystalline phases of various space groups constituted by water-monoglyceride (Dimodan) mixtures. In order to explore the viscoelastic properties of these systems, we use particle tracking of probe colloidal particles suitably dispersed in the liquid crystals and monitored by diffusing wave spectroscopy. The identification of the various liquid crystalline phases was separately carried out by small-angle X-ray scattering. The restricted motion of the particles was monitored and identified by the decay time of intensity autocorrelation function and the corresponding time-dependent mean square displacement (MSD), which revealed space group-dependent behavior. The characteristic time extracted by the intersection of the slopes of the MSD at short and long time scales, provided a characteristic time which could be directly compared with the relaxation time obtained by microrheology. Further direct comparison of microrheology and bulk rheology measurements was gained via the Laplace transform of the generalized time-dependent MSD, yielding the microrheology storage and loss moduli, $G'(\omega)$ and $G''(\omega)$, in the frequency domain ω. The general picture emerging from the microrheology data is that all liquid crystals exhibit viscoelastic properties in line with results from bulk rheology and the transition regime (elastic to viscous) differs according to the specific liquid crystal considered. In the case of the lamellar phase, a plastic fluid is measured by bulk rheology, while microrheology indicates viscoelastic behavior. Although we generally find good qualitative agreement between the two techniques, all liquid crystalline systems are found to relax faster when studied with microrheology. The most plausible explanation for this difference is due to the different length scales probed by the two techniques: that is, microscopical relaxation on these structured fluids, is likely to occur at shorter time scales which are more suitably probed by microrheology, whereas bulk, macroscopic relaxations occurring at longer time scales can only be probed by bulk rheology.

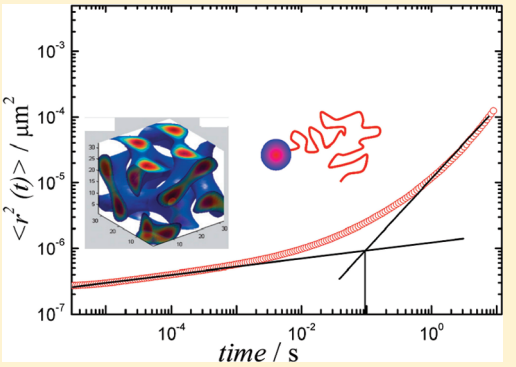

1. INTRODUCTION

A multitude of different types of lyotropic liquid crystals can be formed by the self-assembly of surfactants[1,2] or lipids[3,4] in the aqueous environment, depending on the concentration, temperature, length, and degree of unsaturation of the hydrocarbon chain. Additionally, nonaqueous systems can also form lyotropic liquid crystals.[5] The most commonly found lyotropic liquid crystals are lamellar phases (crystalline, L_c and amorphous, L_α), hexagonal phase (H_{II}), discontinuous or micellar cubic phase (*Fd3m*), and bicontinuous cubic phases (*Ia3d*, *Pn3m*, *Im3m*).[6] These liquid crystals show fascinating viscoelastic properties, which make them suitable in the industrial applications, such as dispersion technology, cosmetics, foods, fertilizers, minerals, encapsulation systems, and so on.[7−11] The bulk rheology of lyotropic liquid crystals has been documented in a number of contributions,[10−18] and it shows an interesting complex behavior and viscoelastic properties. Mezzenga et al.[15] studied binary water-monoglyceride systems, which form two lamellar phases, two bicontinuous phases, and a reverse hexagonal phase depending on the composition and temperature. In that work, the relaxation spectrum and viscoelastic properties were studied at different time-scales, although the limitations of conventional rheology restricted the accessible frequency domain.

Recently, particle tracking microrheology (PTM) technique has attracted a great deal of interest in soft condensed matter as a viable technique to study the viscoelastic properties of soft materials at various length scales and a much extended frequency window. In particular, very low frequencies are in principle accessible without the need of extremely long measurement times, and frequencies as high as 10^4 rad/s are accessible without those inertia problems, which in microrheology start to affect results only beyond 10^5 rad/s.[19−21] PTM relies on the direct or indirect measurement of the mean square displacement (MSD) of probe colloidal particles added to the system to be investigated.[22,23]

The use of PTM has been already employed to characterize emulsions, suspensions, paints, wormlike micelles, etc.[20−28]

Received: October 6, 2010
Revised: March 30, 2011
Published: April 21, 2011

To our knowledge, however, there are only a few reports on the microrheology of lyotropic liquid crystals,[29−31] and these are essentially restricted to the lamellar phase. However, due to the extended accessible frequency domains, it is expected that PTM can also provide additional valuable information over traditional bulk rheology for other classes of mesophases.

In this work, we present a comprehensive study on the microrheology of different types of lyotropic liquid crystals in binary systems of water-monoglycerides (Dimodan). We used diffusing wave spectroscopy to follow the MSD of probe colloidal particles dispersed in the liquid crystals and we extract microrheology information to compare them with bulk rheology. Part of the novelty of this work resides on the great variety of rheological regimes explored by the same single system studied, which is unique to lyotropic liquid crystals, and thus the possibility to compare PTM and bulk rheology in a vast spectrum of viscoelasticity.

2. EXPERIMENTAL SECTION

2.1. Materials. Dimodan U/J was a generous gift from Danisco (Brabrand, Denmark) and was used as received. It contains more than 96 wt % monoglycerides of mixed aliphatic lengths as previously reported.[15] In what follows, it will then be simply referred to as monoglyceride (MG). The same batch was used for all of the measurements carried out in the present work. Milli-Q filtered water was used throughout the experiments. Polystyrene particles (10 wt % in water) were purchased from Polysciences Europe.

2.2. Methods. *2.2.1. Sample Preparation.* First, water and monoglyceride were inserted into vials in the desired compositions and sealed and mixed by means of cyclic heating (up to 80 °C for a few seconds) and vortex-aided vibrations. Once homogeneous mixing was achieved, the vials were cooled to room temperature. Capillaries for SAXS measurements were then filled with and sealed by epoxy resin. Samples for DWS measurements were further loaded with polystyrene particles (diameter 640 nm, 1.5 wt % polystyrene particles) and the probe particles were dispersed in the liquid crystals by means of vortexing. The sample was finally transferred into 5 mm quartz vials for DWS measurements.

2.2.2. Small-Angle X-ray Scattering (SAXS). Small-angle X-ray scattering was used to assess the liquid crystals structure. Experiments were conducted on 1.5 mm thick capillaries and exposed to a Rigaku microfocused X-rays radiation of 0.154 nm wavelength. The data were collected in a two-dimensional argon-filled detector. The applied voltage and filament current were 45 kV and 0.88 mA, respectively. The structure of the liquid crystals were identified by the peak position, namely, L_α (1:2:3...), H_{II} (1:$\sqrt{3}$:$\sqrt{4}$...), *Ia3d* ($\sqrt{6}$:$\sqrt{8}$:$\sqrt{14}$...), and *Pn3m* ($\sqrt{2}$:$\sqrt{3}$:$\sqrt{4}$...), respectively.[15] Depending on the liquid crystal structures, samples were kept at the desired temperature up to 10−30 min before measurements.

2.2.3. DWS Measurements. Experimental set up and data analysis technique were used as described in the literature.[28] DWS measurements were carried out in a transmission mode with a commercial DWS apparatus (LS Instruments). Samples were contained in a flat glass cell with an optical path length of 5 mm and placed in the sample holder. A 683 nm laser was used as the light source (40 mW) and transmitted light was collected on a photomultiplier. For long correlation times, we used the multispeckle echo technique, as described in refs 32 and 33. The detected intensity autocorrelation function was determined with a digital correlator and the electric field autocorrelation function ($g_2(t) - 1$) was determined. The temperature was controlled with a Peltier temperature controller at desired temperature (±0.2 °C). Polystyrene particles (diameter 640 nm) were used as the tracking probe. Samples were maintained 15 min at the required temperature prior to measurements. The sample cells (5 mm thickness) were purchased from Hellma.

In order to check the validity of the multiple scattering regime needed to fulfill DWS analysis, we have determined the value of l^* for each sample by comparing the transmission with that of a reference sample (PS colloidal suspension of known sizes at 1.5 wt %), which gave a $l^* \approx 257 \pm 3\ \mu$m. The cell used was always large enough to maintain $L/l^* > 8-10$, which is in the range of diffusive motion.[34] Byeong and Furst[35] noticed that particle traces with sizes larger than the system mesh size, do not alter the data and that the system behavior then becomes size-independent, whereas smaller particle size does affect the measurements. Since the polystyrene probe particles herein used a diameter much larger than the interlayer spacing or the of the bilayer thickness, no influence on lattice parameter with the inclusion of particles was found (see Supporting Information S1, S2). Furthermore, because of the low amount of probe particles (<1.5 wt %) particle interactions were also found to be negligible.

2.2.4. Bulk Rheological Measurement. To compare microrheology and bulk rheology, bulk rheology was carried out on a stress-controlled rheometer (ARES 2000) using cone−plate geometry (40 mm diameter with cone angle 2°). Samples were homogenized and kept in a thermostatted bath before measurements. Dynamic sweep measurements were performed in the linear viscoelastic regime, as determined by dynamic strain sweep measurements. A sample cover provided with the instrument was used to minimize the change in sample composition by evaporation during measurement.

2.3. Diffusing Wave Spectroscopy (DWS). *2.3.1. Theoretical Background.* DWS is, in many respects, similar to dynamic light scattering (DLS), since both techniques follow the temporal fluctuations of intensity of a speckle of scattered light. This fluctuation reflects the dynamics of the scattering particles.[36] In contrast to DLS, however, DWS operates in a highly turbid medium (multiple scattering) and interprets the photon path through the sample as a diffusive process. Briefly, DWS measures the intensity autocorrelation function of scattered light, $g_2(t)$, as a function of time. Light scattered from the system is an average of several possible multiple scattering diffusive events. One can then calculate the time-averaged autocorrelation function of the scattered electric field ($g_2(t) - 1$) as follows:[37,38]

$$g_2(t) - 1 = \frac{1}{\beta}\left(\int_0^\infty P(s)\exp\left(-\frac{1}{3}k_0^2\langle\Delta r^2(t)\rangle\frac{s}{l^*}\right)\mathrm{d}s\right)^2 \quad (1)$$

where β is a factor determined by the optics set up, $P(s)$ is the probability distribution function of a given path followed by the photon of total length s, s is the path length, $k_0 = 2\pi n/\lambda$, with n the refractive index of the solvent and λ the wavelength of the laser, $< \Delta r^2(t) >$ is the mean square displacement (MSD) of the scatters, and l^* is the photon transport mean free path which depends directly on the sample. The l^* of the sample is calculated directly by comparing the count rate (CR) of a reference sample as follows:

$$l^* = l^*_{\mathrm{REF}} \times \frac{CR_{\mathrm{SAMPLE}}}{CR_{\mathrm{REF}}} \quad (2)$$

The MSD can be extracted from $g_2(t) - 1$ inverting eq 1, with known $P(s)$ (which depends on the sample and on the geometry of the experimental setup). The slope of the log−log plot of the MSD vs time (via an exponent p) yields direct information on the type of motion: when $p = 0$ the fluid is elastic and the motion is confined, and when $p = 1$, the motion is purely Brownian and $\langle\Delta r^2(t)\rangle = 6Dt$, with D being the diffusion coefficient.[39,40] For the microrheological analysis, we use the Laplace transformation of the MSD (fitted by a polynomial of order 7) to extract the storage and loss moduli $G'(\omega)$ and $G''(\omega)$ as described by Mason:[40,41]

$$G(s) \approx \frac{k_B T}{\pi a\langle\Delta r^2(t)\rangle\Gamma\lfloor 1 + (\partial \ln\langle\Delta r^2(t)\rangle\rfloor}\Big|_{t=1/s} \quad (3)$$

where, Γ is the gamma function.

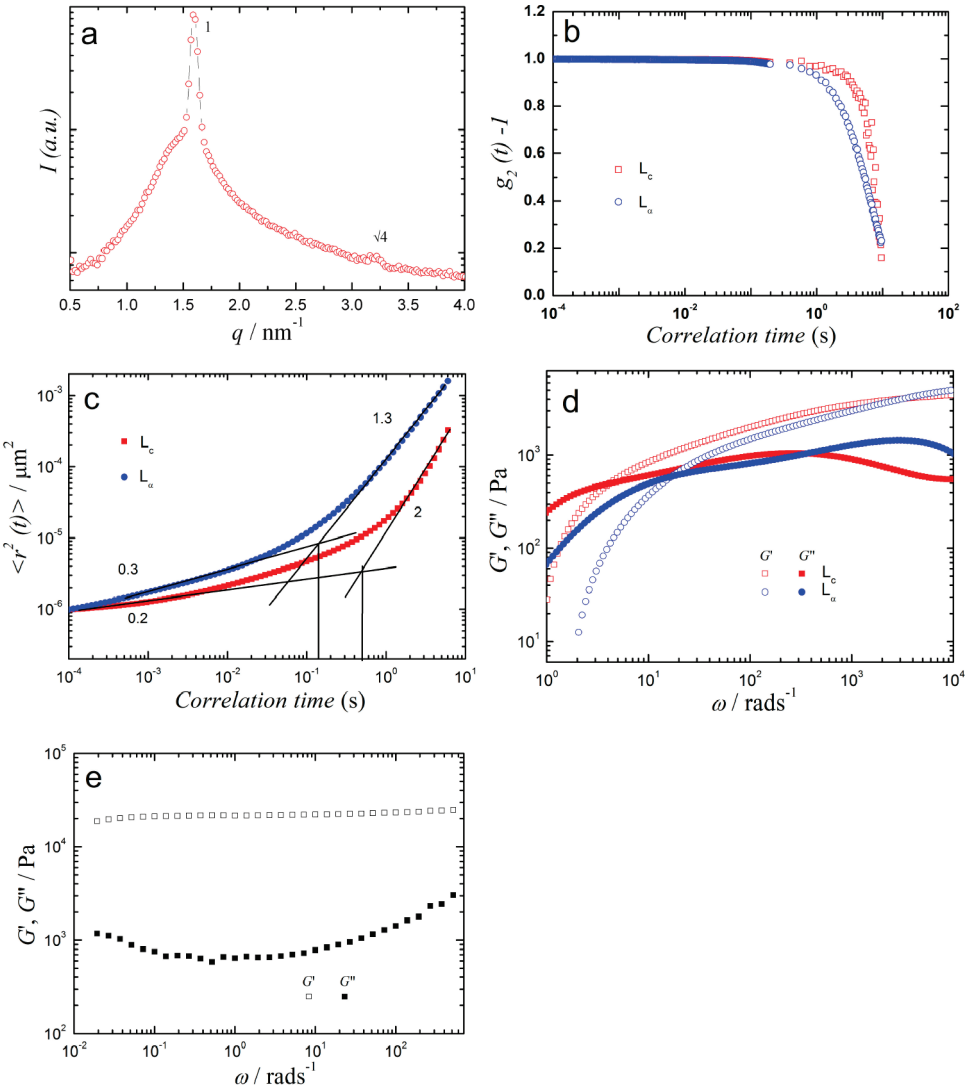

Figure 1. (a) SAXS spectrum of lamellar liquid crystal (L_α) (10 wt % water at 30 °C), (b) normalized autocorrelation function for L_c (5 wt % water, red symbols) and L_α (10 wt % water, blue symbols), (c) mean square displacement of the L_c and L_α phases, (d) microrheology of the L_c and L_α phases derived from Laplace transform of the MSD (e) bulk rheology of the lamellar phase (L_α). The intersection of the lines in part c indicates a characteristic transition time from elastic to viscous state. All measurements were carried out at 30 °C.

3. RESULTS AND DISCUSSION

The binary phase diagram of the monoglyceride (MG)-water has been already well documented[6,15] and we will not present a detailed phase diagram determination here. However, because we are using a commercial grade monogyceride system (which can present small compositional variation from batch to batch), we will assess by SAXS each individual liquid crystalline phase investigated.

3.1. Microrheology of lamellar liquid crystals (L_c, L_α). It is known that in a monoglyceride-water system, two different types of lamellar phases exist: one in which the alkyl tails have crystallized (L_c), and another with amorphous tails (L_α). In this work, we indeed observed two types of lamellar phases. The SAXS spectrum of the amorphous lamellar phase (L_α) is shown in Figure 1a.

In Figure 1a, the SAXS spectrum clearly shows two peaks ($1:\sqrt{4}$) corresponding to the lamellar liquid crystal and bear a typical scattering profile as already reported in the literature.[15,42,43] The rather pronounced background present in the lamellar phase does not allow one to rule out the presence of a coexisting sponge phase, as previously discussed by Glatter et al.[44] and Couvreur et al.[45] However, as is shown in Figure 1e, the bulk rheology of this phase indicates a purely plastic behavior, which then allows one to dismiss the presence of a bicontinuous—and thus viscoelastic—sponge phase. Figure 1b shows the normalized autocorrelation function of both types of lamellar phases. In both the cases, the autocorrelation functions decay at very long time scales and do not reach zero value, indicating nonergodic systems. A closer view of the curves shows a longer decay time for the L_c phase compared to the L_α, certainly due to the crystalline nature of the L_c phase. In Figure 1c, the mean square displacements (MSD) for both phases show a signature of viscoelasticity. At short time scales ($<10^{-2}$ s), the MSD increases slowly, indicating nearly elastic motion; however, at long time scales ($>10^{-1}$ s), the value of the MSD increases steeply, indicating viscous flow. The peculiar super diffusive

dx.doi.org/10.1021/la200116e |*Langmuir* 2011, 27, 6171–6178

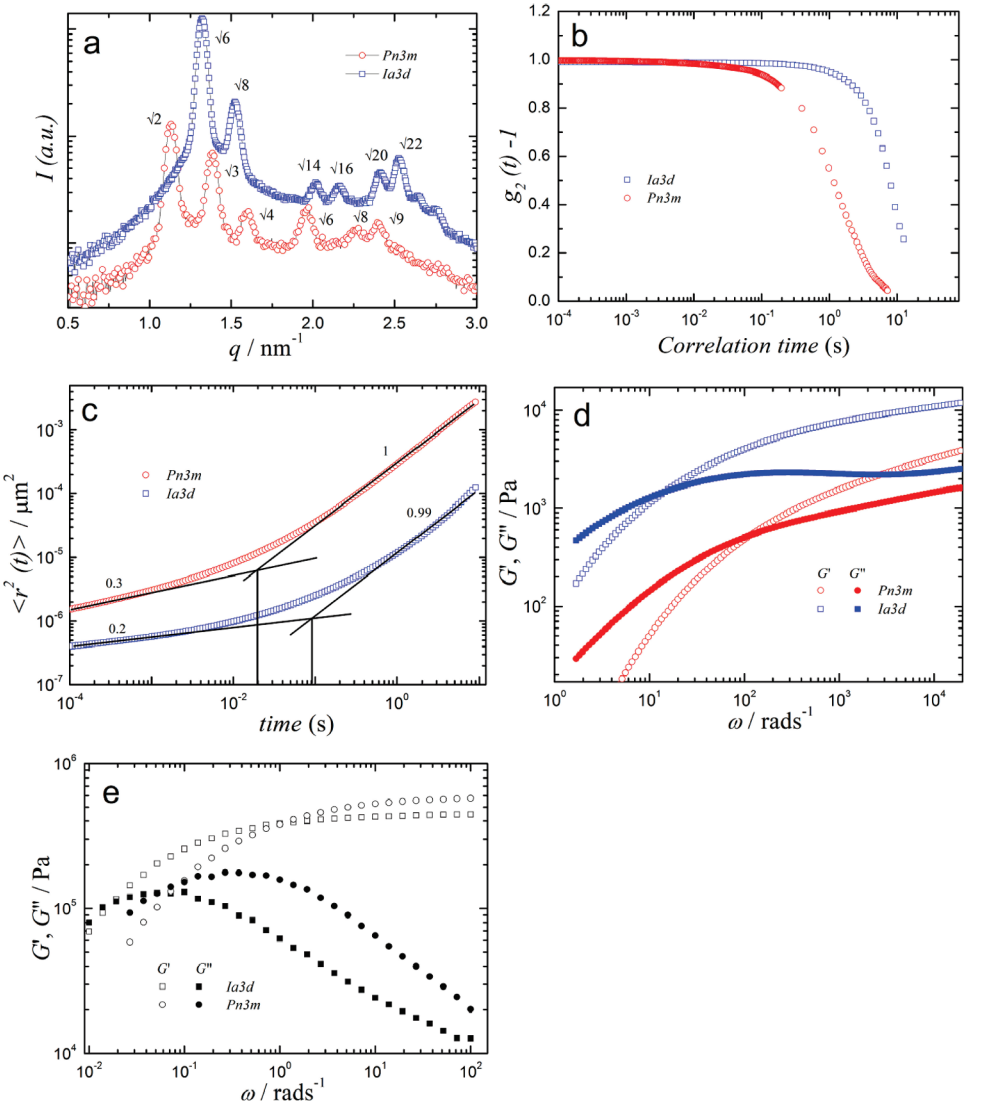

Figure 2. (a) SAXS spectra of bicontinuous cubic phases, *Ia3d* (25 wt % water, 30 °C) and *Pn3m* (35 wt % water, 65 °C), (b) normalized autocorrelation function, (c) mean square displacement, (d) microrheology for the same cubic phases in parts (a) and (e) bulk rheology of cubic phases. The intersection of the lines in part c indicates a characteristic transition time from elastic to viscous regimes.

behavior found for the lamellar phases in the long time scale regime ($1 < p < 2$) is probably due to the plastic nature of the lamellar phase,[15] which can undergo yielding, to which ballistic motion of probe particles can possibly be associated. The evolution of the MSD with time can be interpreted in the following way: at short time scales, the particles are locally trapped within the surrounding mesophase organized in lamellar phases. However, at long time scales, the particles can finally escape from their confined region and have free diffusion.[46] The intersection of the two slopes of the MSD at these two different regimes identifies a characteristic time at which the change in the viscoelastic regime can be clearly identified. It is clear that the relaxation time is longer for L_c phase (0.5 s) compared to L_α phase (0.08 s). This is again in agreement with the decay of the autocorrelation function and reflects, again, the higher rigidity of L_c. In Figure 1d, we show the viscoelastic properties of the two phases as derived from the MSD with Laplace transformation.[41] In both the cases, at low frequency, or long observation times, a fluid-like behavior is found since the loss modulus, G'', dominates over the elastic modulus, G'. At a certain frequency (ω_c), a crossover between the G' and G'' could occurs corresponding to a relaxation time ($\tau_R = 1/\omega_c$), and at frequencies higher than ω_c, G' dominates over G'', indicating elastic or solid-like properties. Consistent with the analysis done above, the relaxation time τ_R of the L_α is shorter by nearly a decade than the one corresponding to the crystalline lamellar phase (L_c), giving $\tau_R = 0.06$ s, 0.25 s for L_α and L_c, respectively. These values are close to those estimated with the slope intercepts of the MSD in Figure 1c.

It becomes highly interesting to compare the information extracted by microrheology with that based on standard bulk rheology, and discuss analogies, differences, and complementary information. Microrheology and bulk rheology have already been compared for a number of soft matter systems.[28,47] However, it remains highly debated and questionable whether a perfect agreement should be expected at all. First of all, in the case of microrheology, any external force is not necessary while in the case of bulk rheology, an applied force/torque is mandatory; second, microrheology probes relaxations at microscopic length

dx.doi.org/10.1021/la200116e |*Langmuir* 2011, 27, 6171–6178

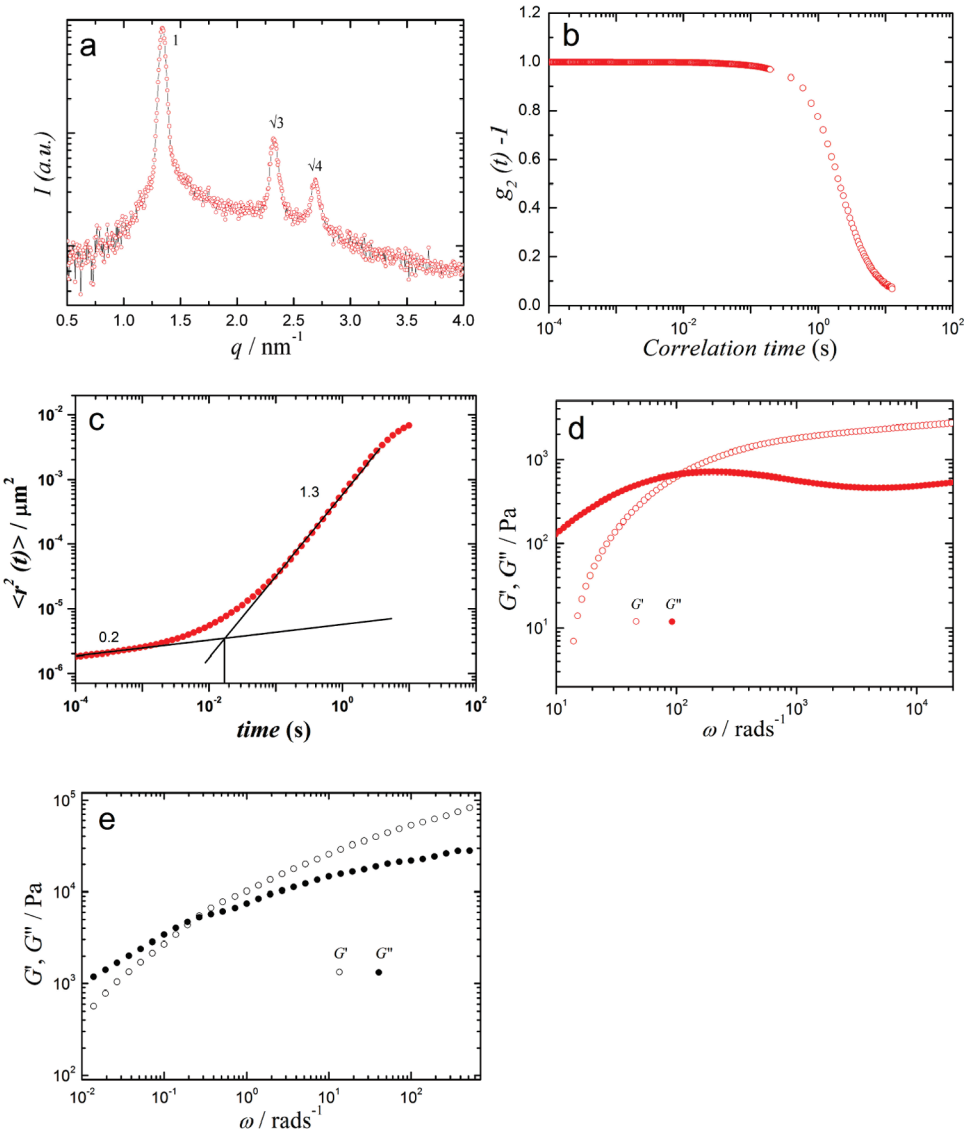

Figure 3. (a) SAXS spectrum, (b) normalized autocorrelation function, (c) mean square displacement, (d) microrheology of the hexagonal lyotropic liquid crystal (H_{II}) observed at 25 wt % water at 65 °C, and (e) bulk rheology. In part c, the intersection of the slopes indicates a characteristic transition time from elastic to viscous regimes.

scales, while bulk rheology gives collective relaxations at the macroscopic level.

In Figure 1e, the bulk rheology frequency scan of the lamellar phase (L_α) is shown. The rheogram is very similar to those reported for lyotropic lamellar phases in previous reports.[15,48] Nonetheless, a pronounced difference with the corresponding microrheology rheogram (Figure 1d) is found. In the bulk rheology, the elastic modulus, G' remains higher than the viscous modulus, G'', throughout the entire frequency window available, consistent with an elastic nature. The steeper increase of the G'' compared to G' at higher frequency indicates dissipation mechanisms, as previously reported.[15] This behavior is consistent with that of a plastic material.[15,49] From the trend of the G' and G'', it is possible to extrapolate that two crossover frequencies locate at (nonobservable) lower and higher frequencies. The low-frequency event would correspond to the transition from viscous to elastic fluid, whereas the high frequency event would be a signature of plastic dissipative events. In the case of microrheology, the behavior observed in a comparable frequency window seems to be much less elastic and more viscous, e.g., that same behavior expected by bulk rheology to occur at very low frequencies. This suggests that microrheology probes faster relaxation mechanisms, and this hypothesis will be further supported by the study of the comparison of the two techniques on the other liquid crystals presented in what follows.

3.2. Microrheology of Bicontinuous Cubic Liquid Crystals (*Ia3d*, *Pn3m*). In previous work, Mezzenga and colleagues[15] showed a wide area of the *Ia3d* and *Pn3m* phases for the water-monoglyceride system. In the present system, we observed the *Ia3d* phase at 25 wt % water and 30 °C and the *Pn3m* at 35 wt % water and 65 °C: the exact *Ia3d*-*Pn3m* boundaries seem to have slightly shifted as a consequence of the different commercial Dimodan batch used. The SAXS spectra for both phases are shown in Figure 2a.

In Figure 2a, it is straightforward to identify the scattering peak positions as $\sqrt{6}$:$\sqrt{8}$:$\sqrt{14}$:$\sqrt{16}$:$\sqrt{20}$:$\sqrt{22}$ for the gyroid

dx.doi.org/10.1021/la200116e |*Langmuir* 2011, 27, 6171–6178

bicontinuous phase (*Ia3d*) and $\sqrt{2}$:$\sqrt{3}$:$\sqrt{4}$:$\sqrt{6}$:$\sqrt{8}$:$\sqrt{9}$ for the double diamond cubic phase (*Pn3m*).[15] Figure 2b shows the normalized autocorrelation function for both systems. In both cases, the correlation function decays at long time scale. A closer view indicates evident differences among the two cubic phases with a decay time longer for *Ia3d* compared to the *Pn3m*. It was already pointed out in previous work that *Ia3d* has higher viscosity than *Pn3m* and longer (bulk) relaxation time,[15] so it is reasonable to expect slower decay for *Ia3d* compared to the *Pn3m*. In the present work, it is possible that temperature provides additional contribution to the decay rate of the *Pn3m*, as the temperature is considerably higher than in the *Ia3d* case. In Figure 2c, the mean square displacement of both *Ia3d* and *Pn3m* is presented. Again, and as expected, one can observe that both phases show nearly elastic behavior at short time scales (MSD shows plateau-like behavior) and purely viscous behavior at long time scales (MSD increases linearly with time). Another observation is that the MSD curve for *Ia3d* is systematically below that of *Pn3m*, indicating higher viscoelasticity for the *Ia3d* crystal. The intersection between the tangents in two different regimes (elastic and viscous) provides, once more, a valuable time period to indicate the transition from the elastic to the viscous regime. Given the higher viscoelasticity of *Ia3d* compared to the *Pn3m*, it comes as no surprise that the crossover regime occurs one decade earlier for the *Pn3m* (10^{-2} s) than *Ia3d* (10^{-1} s), as revealed by the intersection point. In the Figure 2d, the microrheological analysis is shown as derived from Laplace transformation of MSD. In perfect agreement with the analysis of the MSD, in both cases, the viscous, G'', and elastic, G', moduli increase with increasing frequency. At higher frequency, the G' dominates G'' in both cases, indicating the elastic nature of the liquid crystals at high frequencies or short observation times. At the intermediate frequencies, (ω_c), a crossover between G' and G'' occurs, corresponding to a relaxation time $\tau_R = 1/\omega_c$. Remarkably, The relaxation times found by the crossover of G' and G'' are identical to those extracted by the intersect of the slopes in the MSD (Figure 2c), that is 0.01 and 0.1 s for the *Pn3m* and *Ia3d*, respectively. Similarly, the values of G' and G'' are systematically higher at all frequencies for the *Ia3d* compared to the *Pn3m*: again, this confirms the analysis based directly on the MSD and correlation function, indicating higher viscoleasticity in the case of the *Ia3d* cubic phase.

Figure 2e shows the bulk rheology of the bicontinuous cubic phases (*Ia3d* and *Pn3m*). Once again, very good agreement is found with the rheograms reported for the same systems in earlier work.[15] As already discussed in ref 15, the rheogram profile in both bicontinuous cubic phases resemble that of a multiple Maxwell model, with an observable maximum in G'' and a plateau at high frequencies for G'. In both the bicontinuous cubic phases, the elastic, G', and viscous, G'', moduli crossover at a frequency of 0.02 rad/s for *Ia3d* and 0.1 rad/s for *Pn3m*, which indicates relaxation times of 50 and 10 s, respectively. The observed relaxation times in the present system are somehow longer than those reported for similar systems (4.78 s for *Ia3d* and 1.89 for *Pn3m*),[15] which is attributed to the slightly different composition of the commercial formulation used. The corresponding microrheological frequency dependence of G' and G'' (Figure 2d), does show similar behavior, but, once more, the crossover frequencies are found at higher characteristic values yielding relaxation times of 0.1 and 0.01 s for *Ia3d* and *Pn3m*, which are markedly faster than the corresponding ones measured by bulk rheology.

3.3. Microrheology of the Reverse Hexagonal Phase (H_{II}). Although there are several reports describing the bulk rheology of the hexagonal liquid crystals, most of them rely on small frequency windows which cannot comprehensively describe the viscoelastic properties at higher frequencies.[12,15] By using a microrheology approach to study the H_{II} phase, we can assess the high frequency region for this complex fluid as well.

Figure 3a shows the SAXS spectrum of the H_{II} phase with three clearly visible peaks (peak ratio, 1:$\sqrt{3}$:$\sqrt{4}$) identifying the columnar hexagonal phase. In Figure 3b, the autocorrelation function ($g_2(t) - 1$) of the H_{II} phase is shown: at short time scale, a plateau value is visible, indicative of an elastic behavior at these time scales; at longer time scales, however, the correlation function decays down to zero. In Figure 3c, we plot the corresponding MSD versus time. Once again, the time dependence of the MSD provides the expected information: at short time scales, solid-like behavior is found with a very weak time dependence of the MSD with increasing time scale; however, a sharp transition is found to a purely viscous fluid with a linear time dependence of the MSD. If a characteristic transition time is extrapolated by the intersection of the slopes to the two regimes, then a value of 0.02 s is found. Microrheology data of the H_{II} phase is presented in Figure 3d. One can easily note that at low frequencies, G'' dominates G', indicating viscous behavior. With increasing frequencies, the viscous and elastic moduli increase at different rate and at a given frequency (ω_c) they crossover. In the present system, the crossover occurs at 100 rad/s, corresponding to a relaxation time $\tau_R = 1/\omega_c$ of 0.01 s. Once again, remarkably good agreement is found with the transition time obtained upon extrapolation of the slopes of the MSD (Figure 3c). Beyond the crossover frequency, G' reaches a nearly frequency independent plateau, while G'' goes through a minimum and then increases again. This viscoelastic behavior fits well with that of any structured fluid in a broad window of accessible frequencies[50] with viscous conduct at lower frequencies, and elastic nature at higher frequencies. At very high frequencies, the increasing rate of G'' is higher than G', leading to a possible second crossover of G'' and G' (not observed in the present case).

The bulk rheology rheogram (Figure 3e) shows similar features, with a typical viscous behavior at lower frequencies and the elastic nature at higher frequencies. However, the relaxation time is much faster in the case of microrheology (0.01 s) compared to the bulk rheology (3.7 s). In the case of microrheology, a plateau in G' and a minimum in G'' can be observed which are not visible in the bulk rheology due to the narrower frequency window probed. These observations are consistent with those found in the lamellar phase, suggesting that microrheology seems to probe faster relaxation mechanisms as compared to bulk rheology.

A common additional discrepancy found between the bulk rheology and the microrheology is on the value of the storage and loss moduli, where the G' and G'' measured by microrheology are found to be 1 to 2 orders of magnitude lower than those obtained by bulk rheology. This is consistent with previously made observations by one-probe particle tracking microrheology, and two-point particle tracking microrheology generally has to be used to resolve this discrepancy.[51]

3.4. Relaxation Spectra of Liquid Crystalline Phases. As for other types of complex and structured fluids, the description of viscoelastic properties of liquid crystalline phases cannot be comprehensively described by a single relaxation time; quite to the contrary, given the complexity of lyotropic liquid crystals,

several relaxation times should be considered to describe, at best, their rheological behavior. A suitable approach is to consider the relaxation time spectrum, $H(\tau)$, which can be extracted from the dynamical mechanical data $G'(\omega)$ and $G''(\omega)$. In the present work, we have followed this approach and we give a detailed analysis in the Supporting Information.

Here, we also note that the analysis based on relaxation spectra indicate that all liquid crystalline systems are systematically found to relax much more rapidly when studied with microrheology (see the Supporting Information). These findings are supported by similar considerations based on the analysis of the MSD and $g_2(t) - 1$. Because the difference in relaxation times are often of few orders of magnitude, we infer that the sources for these discrepancies have to be found on the very different length scales probed by the two techniques. More specifically, microscopic relaxation of these structured fluids are likely to occur at length scales of the order of their characteristic mesh size (∼nm); consequently, the corresponding shorter time scales are more suitably probed by microrheology ($t \sim \langle r^2 \rangle / D$); on the contrary, bulk, macroscopic relaxations occurring at longer time scales can only be probed by bulk rheology.

These findings are consistent with previous works carried out on different systems. For example, in gel-like dispersions formed by actin and water, it was demonstrated that microrheology probes different length scales with respect to conventional rheology.[52] More recently Pelletier et al.,[51] have compared microrheological measurements on microtubule solutions, as well as composite networks. Although they were able to correct for some discrepancies between the two techniques using two-point microrheology at high frequencies, at time scales on the order of a second, the mismatch could not still not be resolved.

The present work is the first report demonstrating that microrheology and bulk rheology do probe different length scales also in systems in which the mesh size is by several orders of magnitude lower than the probe size, and in a range of viscoelasticity as wide as the one probed in the lyotropic liquid crystals studied here.

4. CONCLUSIONS

We have investigated the microrheological properties of the lyotropic liquid crystals in the binary system of water-monoglyceride (Dimodan) mixtures. The structure of the lamellar (L_α), hexagonal (H_{II}), gyroid (*Ia3d*), and double diamond (*Pn3m*) bicontinuous cubic phases were assessed by small-angle X-ray scattering technique. Microrheological analysis was carried out by probe particle tracking via diffusing wave spectroscopy (DWS). The autocorrelation function, the mean square displacement of the tracer particles, and the storage and loss moduli obtained via the Laplace transform of the mean square displacement were analyzed in the various liquid crystalline phases and compared with the viscoelastic response observable with bulk rheology. Further comparison between the two techniques was carried out by analysis of the corresponding relaxation spectra. All liquid crystalline phases investigated exhibit viscoelastic properties; however, the transition regime from viscous to elastic behavior occurs at a relaxation time that varies according to the liquid crystalline phase considered. These findings are common to both microrheological and bulk rheology investigation. The main difference between the viscoelastic behaviors probed with these two techniques consists on the values of the relaxations times: microrheology, typically yields relaxation times orders of magnitudes lower than those observed by bulk rheology. This is argued to be due to the different time and length scales accessible by the two techniques: microrheology probes microscopical relaxation occurring at very short time scales, while bulk rheology probes macroscopic relaxations occurring at long time scales.

■ ASSOCIATED CONTENT

Supporting Information. SAXS diffractograms with and without probe particles and relaxation spectra. This material is available free of charge via the Internet at http://pubs.acs.org.

■ AUTHOR INFORMATION

Corresponding Author

*Phone: + 41446329140; Fax: + 4144 6321603; E-mail: raffaele.mezzenga@agrl.ethz.ch.

■ ACKNOWLEDGMENT

We are thankful to Prof. Frank Scheffold for scientific discussions about the data analysis and diffusing wave spectroscopy technique.

■ REFERENCES

(1) Mitchell, D. J.; Tiddy, G. J. T.; Waring, L.; Bostock, T.; McDonald, M. P. *J. Chem. Soc. Faraday Trans.* **1983**, *79*, 975.
(2) Li, X.; Kunieda, H. *Langmuir* **2000**, *16*, 10092.
(3) Luzzati, V.; Vargas, R.; Gulik, A.; Mariani, P.; Seddon, J.; Rivas, E. *Biochemistry* **1992**, *31*, 279.
(4) Seddon, J.; Zeb, N.; Templer, R. H.; McElhaney, R. N.; Mannock, D. A. *Langmuir* **1996**, *12*, 5250.
(5) Shrestha, L. K.; Sato, T.; Aramaki, K. *Langmuir* **2007**, *23*, 6606.
(6) Hyde, S. T.; Ericsson, B.; Andersson, S.; Larsson, K. *Z. Kristallogr.* **1984**, *168*, 213.
(7) Krog, N.; Food Emulsifiers and Their Chemical and Physical Properties. In *Food Emulsions*; Friberg, S. E., Larsson, K., Eds.; Marcel Dekker Inc.: New York, 1997; p 141.
(8) Mariani, P.; Rustichelli, F.; Saturni, L.; Cardone, L. *Eur. Biophys. J* **1999**, *28*, 294.
(9) Larrson, K. *Curr. Opin. Colloid Interface Sci.* **2000**, *5*, 64.
(10) Alam, M. M.; Aramaki, K. *Langmuir* **2008**, *24*, 12253.
(11) Mezzenga, R.; Schurtenberger, P.; Burbidge, A.; Michel, M. *Nature Mat.* **2005**, *4*, 729.
(12) Rodriguez, C.; Achariya, D. P.; Aramaki, K.; Kunieda, H. *Colloids Surf. A* **2005**, *269*, 59.
(13) Alam, M. M.; Shrestha, L. K.; Aramaki, K. *J. Colloid Interface Sci.* **2009**, *329*, 366.
(14) Matsumoto, Y.; Alam, M. M.; Aramaki, K. *Colloids Surface A* **2009**, *341*, 27.
(15) Mezzenga, R.; Meyer, C.; Servais, C.; Romoscanu, A. I.; Sagalowicz, L.; Hayward, R. C. *Langmuir* **2005**, *21*, 3322.
(16) Pouzot, M.; Mezzenga, R.; Leser, M.; Sagalowicz, L.; Guillot, S.; Glatter, O. *Langmuir* **2007**, *23*, 9618.
(17) Sagalowicz, L.; Mezzenga, R.; Leser, M. *Curr. Opin. Colloid Interface Sci.* **2006**, *11*, 224.
(18) Ahir, S. V.; Petrov, P. G.; Terentjev, E. M. *Langmuir* **2002**, *18*, 9140.
(19) Mason, T. G.; Weitz, D. *Phy. Rev. Lett.* **1995**, *74*, 1250.
(20) Alexander, M.; Corredig, M.; Dalgleish, D. G. *Food Hydrocolloids* **2006**, *20*, 325.
(21) Vincent, R. R.; Williams, M. A. K. *Carbohydr. Res.* **2009**, *344*, 1863.
(22) Harden, J. L.; Viasnoff, V. *Curr. Opin. Colloid Interface Sci.* **2001**, *6*, 438.

(23) Cohen, I.; Weihs, D. *J. Food Eng.* **2010**, *100*, 366.
(24) Wyss, H. M.; Romer, S.; Scheffold, F.; Schurtenberger, P.; Gauckler, L. *J. Colloid Interface Sci.* **2001**, *240*, 89.
(25) Corredig, M.; Alexander, M. *Trends Food Sci. Tech.* **2008**, *19*, 67.
(26) Giraud, I.; Dantras, E.; Brun, A.; Dihang, H.; Brunel, L.; Bernes, A.; Meunier, G.; Lacabanne, C. *Prog. Org. Coat.* **2009**, *64*, 515.
(27) Willenbacher, N.; Oelschlaeger, C.; Schopferer, M.; Fischer, P.; Cardinaux, F.; Scheffold, F. *Phys. Rev. Lett.* **2007**, *99* (6), 068302.
(28) Oelschlaeger, C.; Schopferer, M.; Scheffold, F.; Willenbacher, N. *Langmuir* **2009**, *25*, 716.
(29) Mizuno, D.; Kimura, Y.; Hayakawa, R. *Phys. Rev. Lett.* **2001**, *87*, 088104.
(30) Mizuno, D.; Kimura, Y.; Hayakawa, R. *Phys. Rev. E* **2004**, *70*, 011509.
(31) Kimura, Y.; Mizuno, D. *Mol. Cryst. Liq. Cryst.* **2007**, *478*, 3.
(32) Zakharov, P.; Cardinaux, F.; Scheffold, F. *Phys. Rev. E.* **2006**, *73*, 011413.
(33) Zakharov, P.; Scheffold, F. *Int. Soc. Opt. Eng.* 2006 (DOI: 10.1117/2.1200609.0397)
(34) Weitz, D. A.; Pine, D. J.; Pusey, P. N.; Tough, R. J. A. *Phys. Rev. Lett.* **1989**, *63*, 1747.
(35) Seok, B.; Furst, E. M. *Langmuir* **2005**, *21*, 3084.
(36) Berne, B. J.; Pecora, R. *Dynamic Light Scattering*; New York: John Wiley and Sons, 1976.
(37) Weitz, D.; Pine, D. J. *Dynamic Light Scattering*; Brown, W., Ed.; Oxford University Press: New York, 1992; Chapter 16.
(38) Khalloufi, S.; Corredig, M.; Alexander, M. *Colloids Surf. B* **2009**, *68*, 145.
(39) Krall, A. H.; Weitz, D. A. *Phys. Rev. Lett.* **1998**, *80*, 778.
(40) Mason, T. G. *Rheol. Acta* **2000**, *39*, 371.
(41) Mason, T. G.; Ganesam, K.; Zanten, J. H.; Wirtz, D.; Kuo, S. C. *Phys. Rev. Lett.* **1997**, *79*, 3282.
(42) Kunieda, H.; Ozawa, K.; Huang, K. L. *J. Phys. Chem. B* **1998**, *102*, 831.
(43) Alam, M. M.; Varade, D.; Aramaki, K. *J. Colloid Interface Sci.* **2008**, *325*, 243.
(44) Freiberger, N.; Moitzi, C.; Campo, L.; Glatter, O. *J. Colloid Interface Sci.* **2007**, *312*, 59.
(45) Angelov, B.; Angelova, A.; Vainio, U.; Garamus, V.; Lesieur, S.; Willumeit, R.; Couvreur, P. *Langmuir* **2009**, *25*, 3734.
(46) Hinner, B.; Tempel, M.; Sackmann, E.; Kroy, K.; Frey, E. *Phys. Rev. Lett.* **1998**, *81*, 2614.
(47) Ubbink, J.; Burbidge, A.; Mezzenga, R. *Soft Matter* **2008**, *4*, 1569.
(48) Alam, M. M.; Armaki, K. *J. Colloid Interface Sci.* **2009**, *336*, 820.
(49) Montalvo, G.; Valiente, M.; Rodenas, E. *Langmuir* **1996**, *12*, 5202.
(50) Ferry, J. D. *Viscoelastic Properties of Polymers*; John Wiley & Sons: New York, 1980.
(51) Pelletier, V.; Gal, N.; Fournier, P.; Kilfoil, M. L. *Phys. Rev. Lett.* **2009**, *102*, 188303.
(52) Liu, J.; Gardel, M. L.; Kroy, K.; Frey, E.; Hoffman, B. D.; Crocker, J. C.; Bausch, A. R. ; Weitz, D. A. *Phys. Rev. Lett.* **2006**, *96*, 118104.